

## Impact of Nano-Cr<sub>2</sub>O<sub>3</sub> Addition on the Properties of Aluminous Cements Containing Spinel

Sasan OTROJ\*

Faculty of Engineering, Shahrekord University, Saman Gate, P.O. Box:115, Shahrekord, Iran

**crossref** <http://dx.doi.org/10.5755/j01.ms.21.1.5211>

Received 13 September 2013; accepted 16 February 2014

In this paper, the effect of nano-Cr<sub>2</sub>O<sub>3</sub> addition on the properties of aluminous cement containing MgAl<sub>2</sub>O<sub>4</sub> spinel was investigated. For this reason, the raw dolomite was used as raw material along with calcined alumina for the preparation of the aluminous cement. Then, the compositions containing different amounts of nano-Cr<sub>2</sub>O<sub>3</sub> particles were fired at 1450 °C and their mineralogical compositions and microstructures were investigated. The setting times of prepared cements were measured after grinding and ball-milling. Besides, the slag resistance of refractory castables containing prepared cements was evaluated. The results showed that nano-Cr<sub>2</sub>O<sub>3</sub> addition has effect on the increasing of spinel and CA<sub>2</sub> and decreasing of CA and C<sub>12</sub>A<sub>7</sub> phases in the cement composition. The decreasing of C<sub>12</sub>A<sub>7</sub> leads to increasing of setting times of cement. Besides, the slag resistance of refractory castables containing prepared cements is improved due to increasing of spinel and decreasing of C<sub>12</sub>A<sub>7</sub> amount in the cement composition.

*Keywords:* aluminate cement, spinel, nano-Cr<sub>2</sub>O<sub>3</sub>, properties, slag resistance.

### 1. INTRODUCTION

MA spinel (MgAl<sub>2</sub>O<sub>4</sub>) is very attractive as refractory material in thermal industries because of its high melting point (2135 °C), low thermal expansion, and considerable hardness, high resistance to chemical attack, favorable chemical stability, and good thermal spalling [1, 2]. Therefore, there is a trend to increase the use of high alumina refractory castables containing MA spinel, because of their higher durability in steel ladles than Al<sub>2</sub>O<sub>3</sub> castables [3, 4]. However, at the present time, the high cost of the sintered and electrofused spinels represents a handicap to more extended development of this kind of refractory materials. Conventionally, MgAl<sub>2</sub>O<sub>4</sub> spinel powders were prepared by solid-state reaction process using oxide MgO and Al<sub>2</sub>O<sub>3</sub> as starting materials [4–7]. In the solid-state process, the mixture of MgO and Al<sub>2</sub>O<sub>3</sub> were usually calcined at temperature as high as 1400 °C–1600 °C to ensure the phase formation. Sintering of such powders would be at extremely high temperatures (> 1700 °C). The spinel mineral, whether artificially added or formed in situ during sintering, is hydraulically inert and does not behave as a binder, but it permits the utilization of refractory castables with a suitable aggregate (tabular alumina, spinel or dead burnt magnesite) up to 1800 °C. It has been reported that the firing of appropriate mixtures of raw dolomite (source of CaO and MgO) and active alumina as primary materials can lead to formation of the aluminous cement containing MA spinel. Therefore, MA spinel (20 %–50 %) in addition to the calcium aluminate hydraulic phases (CA and CA<sub>2</sub>) is formed during the sintering process. On the other hand, the refractoriness of the high alumina cements can be increased substantially, without adversely affecting

their compressive strength, when CaO in the cement clinker is partially substituted by MgO. This type of aluminous cement which contains from 6 % to 13 % MgO is known as spinel-type cement and shows increased thermo mechanical strength and minimal slag attack due to the MA spinel content [7–10]. Therefore, the synthesis of these cements has attracted considerable attention due to practical considerations. Many researches have been conducted to improve the synthetic procedures in order to reduce the production cost of these materials. Generally, the reaction between MgO and Al<sub>2</sub>O<sub>3</sub> begins at about 900 °C, but becomes noticeable only above 1400 °C up to 1600 °C. Effects of different additives on the development of spinel were studied by a number of workers [1, 2, 7–10]. Salt vapors were reported to be useful additives for the development and formation of spinel. Fluorine ion (from AlF<sub>3</sub> or CaF<sub>2</sub>) was found to enhance the solid state reaction synthesis of spinel when it is incorporated in the lattice by replacing oxygen ions. Besides, addition of mineralizers such as, V<sub>2</sub>O<sub>5</sub>, Y<sub>2</sub>O<sub>3</sub>, TiO<sub>2</sub> and B<sub>2</sub>O<sub>3</sub> can help to formation of spinel to some extent. However, use of these additives contaminates the product and restricts its application to low temperatures [11–13].

On the other hand, the use of nanometer oxides as additions to raw material mixtures or as nanometer starting material for the production of ceramic materials is reported in a wide range of literature since several years [14–16]. Nanometer materials are very reactive due to their better homogenization, high specific surface area and therefore the sintering starts at lower temperatures. Consequently, objective of the present work is investigation of nano-Cr<sub>2</sub>O<sub>3</sub> addition on properties of aluminous cements containing MA spinel. Raw dolomite and calcined alumina are used as raw materials with various amounts of nano-Cr<sub>2</sub>O<sub>3</sub> in the preparation of the aluminous cement. Then, the compositions are prepared at 1450 °C using the

\*Corresponding author. Tel.: +98-381-4424438; fax.: +98-381-4424438.  
E-mail address: [sasan.otroj@gmail.com](mailto:sasan.otroj@gmail.com) (S. Otraj)

sintering method. The phase analysis, microstructure and setting times of prepared cements are investigated. Besides, the slag resistance of refractory castables containing prepared cements is evaluated.

## 2. EXPERIMENTAL

### 2.1. Raw materials and compositions

Calcined alumina (source of  $\text{Al}_2\text{O}_3$ ) and highly pure local raw dolomite were used for the preparation of aluminous cement containing spinel ( $\text{MgAl}_2\text{O}_4$ ). The chemical compositions of these starting materials are shown in Table 1.

**Table 1.** Chemical compositions of the raw materials

Oxides	Raw material type	
	Raw dolomite (wt.%)	Calcined alumina (wt.%)
$\text{SiO}_2$	0.51	0.02
$\text{Fe}_2\text{O}_3$	0.27	0.02
$\text{Al}_2\text{O}_3$	0.54	99.60
CaO	31.32	–
MgO	20.16	–
$\text{Na}_2\text{O}$	0.01	0.15
L.O.I	46.82	0.11

The calcined alumina used was a product of Fiberona Co. (HTM 10, India). The raw dolomite used in this investigation (derived from Shahreza regions (Iran)) was finely milled mineral dolomite ( $\text{CaMg}(\text{CO}_3)_2$ ) supplied by Arya Kani Sepahan Co. (Iran). The specifications of raw materials used are shown in Table 2. The nano- $\text{Cr}_2\text{O}_3$  used was a product of NanoAmor Co. which its specifications are shown in Table 3. Specific surface area of the oxide powders was measured by the single-point Brunauer-Emmet-Teller (BET) method using  $\text{N}_2$  gas (Model MS-16, Quantachrome Corp, Suoset, NY, USA). In addition, the mean size of particles was analyzed by a laser particle diameter analyzer (Honeywell Microtrac X-100).

**Table 2.** The specifications of raw materials used

Specification	Raw material	
	raw dolomite	calcined alumina
Density ( $\text{g}/\text{cm}^3$ )	2.84	3.92
$d_{50}$ ( $\mu\text{m}$ )	3.2	4.0
Surface area ( $\text{m}^2/\text{g}$ )	3.1	1.0

**Table 3.** The specifications of nano- $\text{Cr}_2\text{O}_3$  used

Purity (%)	Melting point ( $^\circ\text{C}$ )	Surface area ( $\text{m}^2/\text{g}$ )	$d_{50}$ (nm)
>99	2435	50	60

Considering the  $\text{Al}_2\text{O}_3$ -MgO-CaO ternary system phase diagram [7–10] as well as the chemical composition of dolomite, detailed in Table 1, mixtures of 55 %  $\text{Al}_2\text{O}_3$  and 45 % raw dolomite were prepared in order to obtain

cement samples containing the spinel and calcium aluminates phases such as; CA and  $\text{CA}_2$  for better recognize of nano- $\text{Cr}_2\text{O}_3$  effect on the phase composition. The nano- $\text{Cr}_2\text{O}_3$  was added to the compositions in proportions of 0.5, 1.0 and 1.5 wt %.

### 2.2. Preparation of cement and test methods

The required proportions of the starting materials of each mix were dry blended together, and then wet finely ground in a fused alumina ball mill. After being milled, the prepared mixes were dried and then, formed into briquettes under pressure of  $800 \text{ kg}/\text{cm}^2$ , dried at  $110^\circ\text{C}$  and then fired at  $1450^\circ\text{C}$ , with a soaking time of 5 h [7–10]. The firing was carried out in a electric furnace. The XRD measurements were carried out with a D8ADVANCE, Bruker diffractometer with  $\text{CuK}\alpha$ , Ni-filtered radiation. The proportion of different phases in the cement compositions was determined by semi-quantitative XRD analysis (X'Pert High Score software). Therefore, the d-spacing values related to identified phases are computed. The fracture surface of fired samples after gold coating was evaluated by field emission scanning electron microscope (FE-SEM, JEOL 4010) equipped with an energy-dispersive spectroscope (EDS). The resulting sintered products were crushed, and then finely ground in a fused alumina ball mill to get a cement powder of a suitable fineness. The Blaine surface area of the produced cements was maintained in the range of ( $3500$ – $4000$ )  $\text{cm}^2/\text{g}$ . The setting times of prepared cements were evaluated by Vicat needle test method according to ASTM C191.

### 2.3. Preparation and slag corrosion test of refractory castable

The used raw materials and composition for the preparation of high alumina castable is listed in Table 4.

**Table 4.** Raw materials and composition of alumina refractory castable studied

Raw materials	Source (Type)	wt. %
Tabular Alumina 2–5 mm 1–2 mm 0.5–1 mm 0–0.5 mm $\leq 45 \mu\text{m}$	Alcoa Chemicals, T-60	65
Reactive Alumina	Alcoa Chemicals, CTC-20	15
Cement containing spinel	Prepared cements	20
Additive	S.K.W Polymer, FS 10	0.1

To achieve optimum conditions for castable preparation, some additional factors were also investigated e. g. water/solid ratio and amount of cement in the castable composition. Accordingly, the test method (good-ball in hand ASTM C860) is used for the determination of castable water content and consistency. The obtained results indicated that the water demanded for castable having the required workability was 5 %. The castables for the crucible corrosion tests were cast in metal moulds and were cured at room temperature in airtight containers for 24 h and then dried at  $110^\circ\text{C}$  for another 24 h before

firing. All the specimens had the following dimensions: 110 mm × 110 mm × 80 mm with a diameter of 40 mm and holes 55 mm deep. The laboratory crucible tests were performed independently with a fixed amount of slag (60 g, C/S = 2.6) in each crucible. The slag was provided by steel plants Zobe ahan (Isfahan, Iran). The castables were fired for 5 h at 1650 °C in a laboratory electric furnace and later crucibles were cross-sectioned perpendicular to their diameter. By comparing the respective areas (before and after the attack) via optical microscopic evaluations, it was possible to evaluate the damage on each of the designed compositions.

### 3. RESULTS AND DISCUSSION

#### 3.1. The effect of nano-Cr<sub>2</sub>O<sub>3</sub> addition on the phase composition

The XRD results of prepared cements containing different amounts of nano-Cr<sub>2</sub>O<sub>3</sub> after firing are shown in Fig. 1.

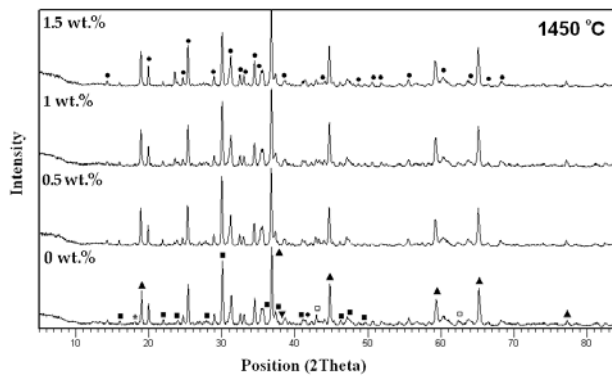


**Fig. 1.** The XRD results of prepared cements by use of different amounts of nano-Cr<sub>2</sub>O<sub>3</sub> after firing ■ – CA, ● – CA<sub>2</sub>, \* – C<sub>12</sub>A<sub>7</sub>, ▲ – spinel, □ – periclase, ▼ – corundum

In all the cement compositions after firing, CaO·Al<sub>2</sub>O<sub>3</sub> (CA), CaO·2Al<sub>2</sub>O<sub>3</sub> (CA<sub>2</sub>), 12CaO·7Al<sub>2</sub>O<sub>3</sub> (C<sub>12</sub>A<sub>7</sub>) and spinel phases are formed as observed in the XRD pattern shown in Fig. 1. Generally, raw dolomite is decomposed into CaO and MgO with increasing of temperature. Then, these oxides are reacted with Al<sub>2</sub>O<sub>3</sub> which, can lead to formation of calcium aluminates and spinel phases. Besides, very low contents of corundum (Al<sub>2</sub>O<sub>3</sub>) as remaining raw material and resultant periclase (MgO) of dolomite decomposition exist. The *d*-spacing values related to identified phases (Fig. 1) are shown in Table 5.

**Table 5.** The *d*-spacing values related to indentified phases in Fig. 1

Phase	2θ (degree)	d-spacing (Å)
CA	30.083	2.97067
CA <sub>2</sub>	25.391	3.50796
C <sub>12</sub> A <sub>7</sub>	18.057	4.91285
Spinel	36.843	2.43962
Periclase	42.917	2.10736
Corundum	37.797	2.38019

The proportion of the different phases in the cement compositions was determined by quantitative XRD analysis. The results are shown in Fig. 2 as a function of nano-Cr<sub>2</sub>O<sub>3</sub> content used in the cement composition.

The results show that the contents of CA and C<sub>12</sub>A<sub>7</sub> phases in the cement composition are decreased with increasing of nano-Cr<sub>2</sub>O<sub>3</sub>. On the other hand, the contents of other phases such as; CA<sub>2</sub> and spinel are increased with the addition of nano-Cr<sub>2</sub>O<sub>3</sub>. Therefore, it can be concluding that the nano-Cr<sub>2</sub>O<sub>3</sub> addition has great effect on the formed phases in the cement composition.

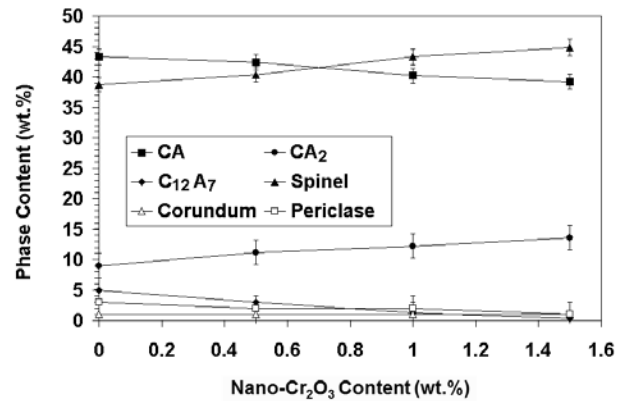


**Fig. 2.** The effect of nano-Cr<sub>2</sub>O<sub>3</sub> content on the content of formed phases in the cement composition after firing

Generally, the mono-calcium aluminate (CA) is the most important component of calcium aluminate cement and has a relatively high melting point (1600 °C). Besides it develops the highest strength among the other phases and then, it has an important role on the improvement of the mechanical strength of refractory cements. Usually, the CA formation takes place at 950 °C. Besides, between 1000 °C and 1100 °C the expansile and exothermic reaction of spinel formation occurs. On the other hand, in the 1000 °C–1200 °C temperature range, CA reacts with alumina to form CA<sub>2</sub> [7–10]. The researchers [7, 8] were shown that the amount of remaining raw materials is considerably decreased with increasing of firing temperature and the complete solid state reactions in these cements are mostly occurred after firing at 1450 °C. Besides, the three main phases of these cements (CA, spinel and CA<sub>2</sub>) are formed at 1450 °C. On the other hand, the C<sub>12</sub>A<sub>7</sub> phase (mayenite) has the lower melting point (1415 °C–1495 °C) among the other formed phases in cement composition. With respect to the results, mayenite significantly is decreased with addition of nano-Cr<sub>2</sub>O<sub>3</sub>. Therefore, the service temperature of these refractory cements can shift to higher temperatures with addition of nano-Cr<sub>2</sub>O<sub>3</sub>. Due to similar crystal structure (hexagonal) and ions with similar electric charge, Cr<sub>2</sub>O<sub>3</sub> dissolves in the Al<sub>2</sub>O<sub>3</sub> structure and solid solution forms. Therefore, Cr<sup>3+</sup> ions show preference to substitute for Al<sup>3+</sup> ions at the octahedral sites. Hence, there is the lattice distortion caused by this substitution because of the difference between ionic radii: 0.62 Å and 0.53 Å for Al<sup>3+</sup> and Cr<sup>3+</sup>, respectively. Therefore, this substitution causes lattice expansion in the structure. Besides, no charge compensation is needed, since electrical charges of both ions are equal [13]. However, lattice expansion causes

higher diffusion coefficients of cations in the structure. Hence, nano-Cr<sub>2</sub>O<sub>3</sub> can enhance the amount of spinel and CA<sub>2</sub> phase through the increasing of diffusion coefficients. Besides, nano-Cr<sub>2</sub>O<sub>3</sub> can be considered as seeds for formation of spinel and CA<sub>2</sub> phases. With substitution of Al<sup>3+</sup> cation by Cr<sup>3+</sup> in the structure the spinel peaks can shift to smaller angles. For further investigation the displacement of spinel peak concerning to [311] plane was studied. In Fig. 3 the effect of 1.5 wt.% nano-Cr<sub>2</sub>O<sub>3</sub> addition on the displacement of spinel peak concerning to [311] plane are shown after firing at 1450 °C.

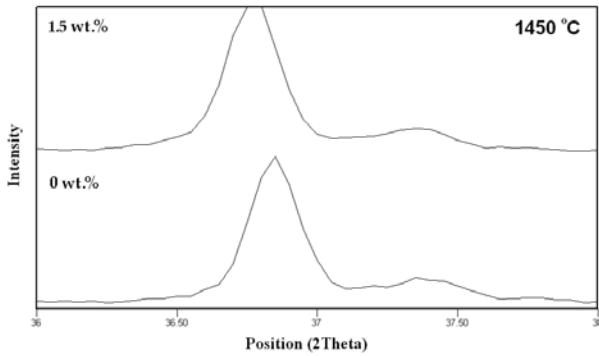


**Fig. 3.** The effect of 1.5 wt.% nano-Cr<sub>2</sub>O<sub>3</sub> addition on the displacement of spinel peak concerning to [311] plane after firing

Fig. 3 clearly shows the spinel peak was shifted to lower angles by nano-Cr<sub>2</sub>O<sub>3</sub> addition. Therefore, nano-Cr<sub>2</sub>O<sub>3</sub> can dissolve in the structure and then, substitution of Al<sup>3+</sup> cation by Cr<sup>3+</sup> takes place.

### 3.2. The effect of nano-Cr<sub>2</sub>O<sub>3</sub> addition on the microstructure

The microstructure of cement composition without nano-Cr<sub>2</sub>O<sub>3</sub> addition after firing at 1450 °C is presented in Figs. 4 and 5.

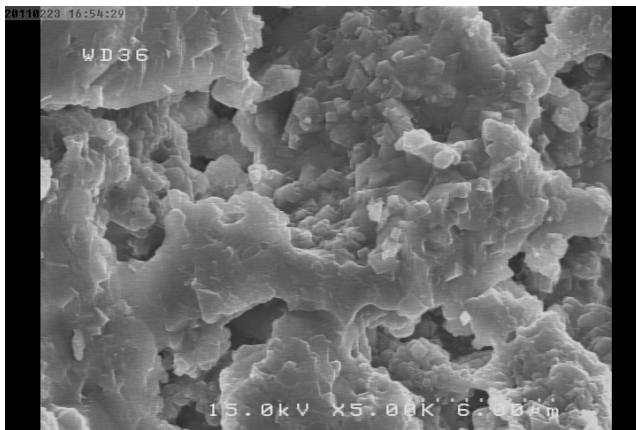


**Fig. 4.** SEM photomicrograph of fired cement composition without nano-Cr<sub>2</sub>O<sub>3</sub>

As it can be seen, the microstructure of these cements is porous and contains the crystalline phases with different grains size. A portion of pores in the microstructure are produced via thermal decomposition of raw dolomite used in the cement composition. According to XRD results of Fig. 1, the present phases in cement composition without nano-Cr<sub>2</sub>O<sub>3</sub> addition after firing at 1450 °C contain CA, CA<sub>2</sub>, C<sub>12</sub>A<sub>7</sub> and MA spinel that linked together via sintering process.

CA, CA<sub>2</sub>, C<sub>12</sub>A<sub>7</sub> and MA spinel that linked together via sintering process. CA presents a globular morphology while spinel phase is seen as aggregates with some cluster of cubic shape crystals. Micrograph of a fracture of the cement after firing shows globular crystals of CA<sub>2</sub> that give a cohesive microstructure.

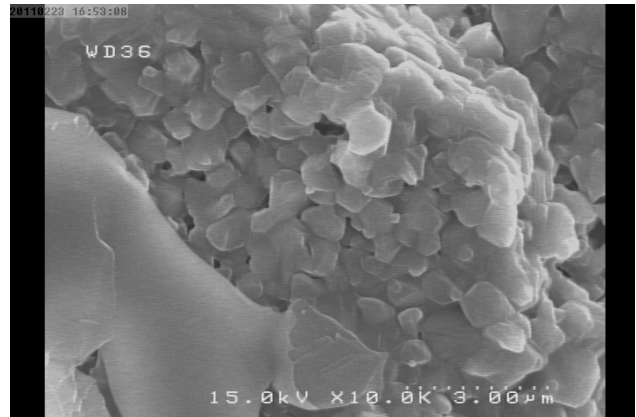


**Fig. 5.** SEM photomicrograph of fired cement composition without nano-Cr<sub>2</sub>O<sub>3</sub>

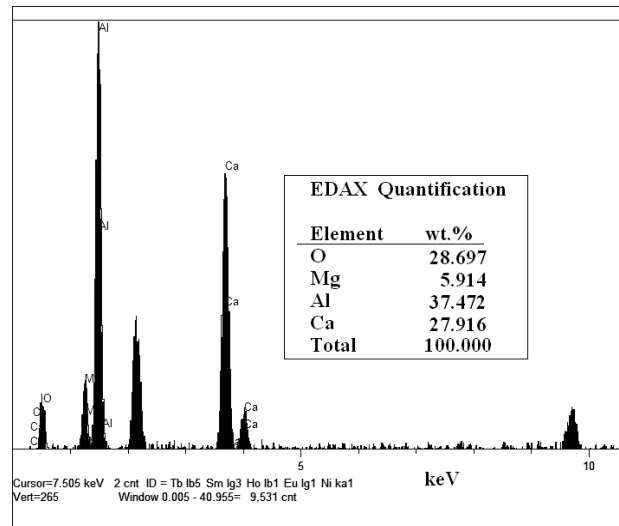


**Fig. 6.** The SEM/EDX analysis of CA phase

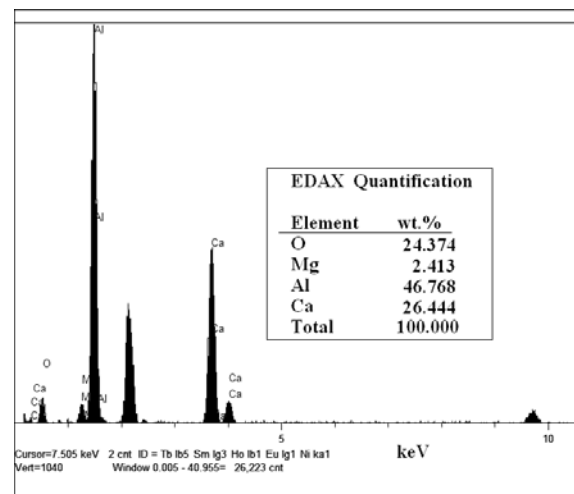


**Fig. 7.** The SEM/EDX analysis of CA<sub>2</sub> phase

To distinguish between CA and CA<sub>2</sub> EDS analyses were necessary because both phases present similar contrast. The SEM/EDX analysis of CA and CA<sub>2</sub> phases are presented in Figs. 6 and 7.

Examination of the fracture surface of the prepared cements by SEM showed that the mayenite possesses the pseudomorphic appearance Figs. 8, 9 and 10 demonstrate the microstructure of cement composition containing 1.5 wt. % nano-Cr<sub>2</sub>O<sub>3</sub> after firing.

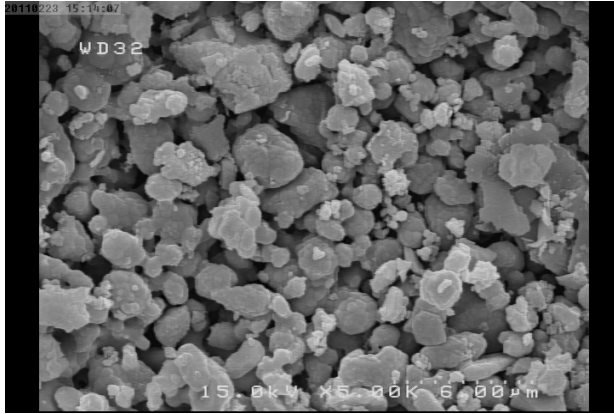


Fig. 8. SEM photomicrograph of fired cement composition containing 1.5 wt. % nano-Cr<sub>2</sub>O<sub>3</sub>

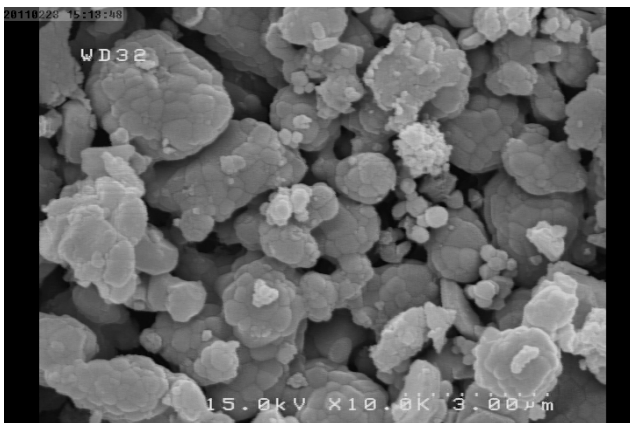


Fig. 9. SEM photomicrograph of fired cement composition containing 1.5 wt. % nano-Cr<sub>2</sub>O<sub>3</sub>

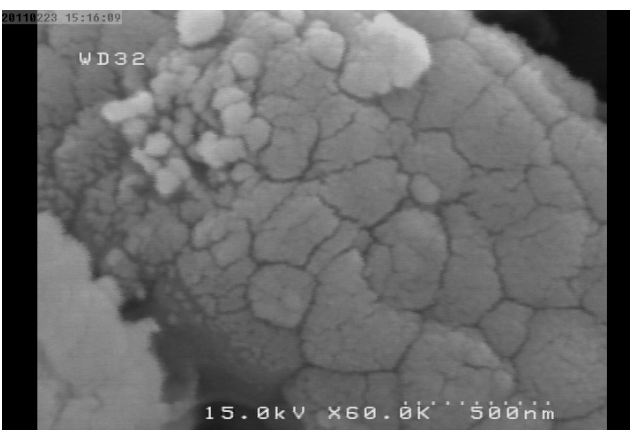


Fig. 10. SEM photomicrograph of fired cement composition containing 1.5 wt. % nano-Cr<sub>2</sub>O<sub>3</sub>

With microstructural evaluation of cement composition containing 1.5 wt. % nano-Cr<sub>2</sub>O<sub>3</sub>, one can see that higher porosity is produced in the microstructure and

then, porous crystalline structure is formed. As shown in XRD results of Fig. 1, the microstructure of cement composition containing 1.5 wt. % nano-Cr<sub>2</sub>O<sub>3</sub> after firing comprises of CA, CA<sub>2</sub>, spinel. Hence, the mayenite phase was not formed in the composition.

As stated above, mayenite has the lower melting point among the other formed phases in cement composition. Therefore, cement composition without nano-Cr<sub>2</sub>O<sub>3</sub> addition after firing at 1450 °C contains amorphous phase which leads to filling of porosity in the structure. Besides, the microstructural analysis of cement composition containing 1.5 wt. % nano-Cr<sub>2</sub>O<sub>3</sub> shows higher amounts of cubic spinel crystals in comparison with compositions without nano-Cr<sub>2</sub>O<sub>3</sub>. The other obvious characteristic in these Figures is that there are very fine micro-cracks on the surface of particles. As stated above, the substitution of Al<sup>3+</sup> cation by Cr<sup>3+</sup> in the structure takes place and this substitution causes lattice distortion and lattice expansion in the structure. High anisotropic volume expansion of structure can lead to micro-crack formation in the particles.

Besides, this substitution causes further mismatch between the elastic modulus of different phases which, probably leads to formation of micro-cracks. These micro-cracks can help to better crushing and then finely grinding of produced cement in the ball mill. The SEM/EDX analysis of particles containing micro-cracks on their surface is presented in Fig. 11. This analysis proves the existence of Cr<sup>3+</sup> in cement particles.

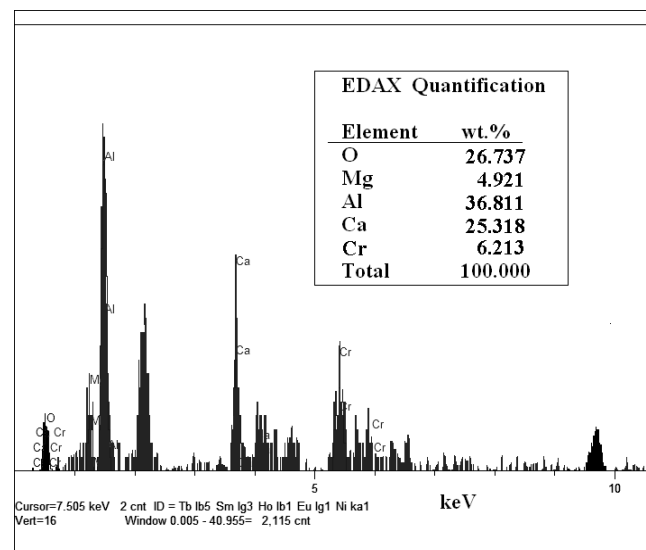


Fig. 11. The SEM/EDX analysis of CA<sub>2</sub> phase

### 3.3. The effect of nano-Cr<sub>2</sub>O<sub>3</sub> addition on the setting times

The relation between the different amounts of nano-Cr<sub>2</sub>O<sub>3</sub> and the setting times of prepared cement pasts are shown in Fig. 12.

The results show that the setting times of prepared cement pastes are increased with addition of nano-Cr<sub>2</sub>O<sub>3</sub>. Generally, setting times of hydraulic cement depend on the phase composition, fineness of the cement and additives. C<sub>12</sub>A<sub>7</sub> phase has rapid initial and final setting times. Besides, CA<sub>2</sub> is a secondary phase in calcium aluminate cement and is more refractory than CA but takes a long time to set due to its low hydraulic activity. Hence, setting

times are affected by the ration of CA/CA<sub>2</sub> and also CA/C<sub>12</sub>A<sub>7</sub> [4, 7–10]. According to XRD results (Fig. 2), the cement without nano-Cr<sub>2</sub>O<sub>3</sub> has noticeably content of C<sub>12</sub>A<sub>7</sub> phase in its composition. Hence, because of rapid initial and final setting times of C<sub>12</sub>A<sub>7</sub> phase, the cement past without nano-Cr<sub>2</sub>O<sub>3</sub> has rapid initial and final setting times in comparison with cement pastes containing nano-Cr<sub>2</sub>O<sub>3</sub>. On the other hand, the contents of CA and C<sub>12</sub>A<sub>7</sub> phases in the cement composition are decreased with increasing of nano-Cr<sub>2</sub>O<sub>3</sub>. Therefore, the setting times of prepared cement pastes are delayed with addition of nano-Cr<sub>2</sub>O<sub>3</sub>.

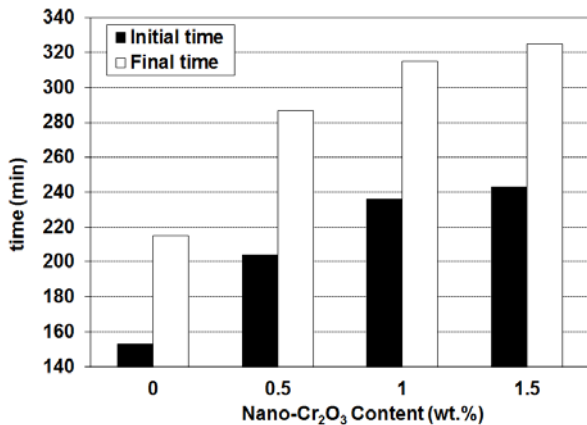


Fig. 12. The relation between different amounts of nano-Cr<sub>2</sub>O<sub>3</sub> and setting times of prepared cement pastes

### 3.4. Evaluation of slag resistance

In Fig. 13, the effects of the attack by the slag on the castables prepared by cement containing 1.5 wt. % nano-Cr<sub>2</sub>O<sub>3</sub> and without it are shown.

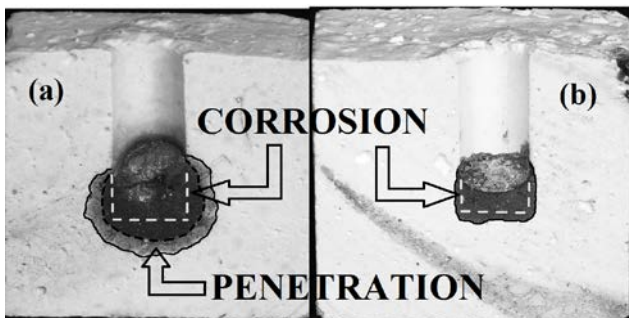


Fig. 13. Schematic diagram of the interior of the crucibles showing the extent of corrosion and penetration slag; a – without nano-Cr<sub>2</sub>O<sub>3</sub>; b – containing 1.5 wt. % nano-Cr<sub>2</sub>O<sub>3</sub>

As it can be seen, the corrosion and penetration by the molten slag decrease with addition of nano-Cr<sub>2</sub>O<sub>3</sub>. As stated above, the mayenite phase has the lower melting point among the other formed phases in cement composition. With respect to the XRD results (Fig. 1), the amount of mayenite significantly is decreased with addition of nano-Cr<sub>2</sub>O<sub>3</sub>. Therefore, the service temperature of these refractory castables containing this type of cement can shift to higher temperatures with addition of nano-Cr<sub>2</sub>O<sub>3</sub>. On the other hands, the refractory cement containing 1.5 wt. % nano-Cr<sub>2</sub>O<sub>3</sub> has higher spinel phase in

its composition. Normally, Mn<sup>2+</sup>, Fe<sup>2+</sup> and Fe<sup>3+</sup> cations in the slag melt are absorbed by spinel to form a solid solution. Hence, the residual molten liquid becomes rich in SiO<sub>2</sub> and increases its viscosity and then, penetration suppresses [1–4, 17]. Therefore, the refractory castable containing cement with 1.5 wt. % nano-Cr<sub>2</sub>O<sub>3</sub> has higher slag penetration resistance in comparison with cement containing without nano-Cr<sub>2</sub>O<sub>3</sub>.

## 4. CONCLUSIONS

The effect of nano-Cr<sub>2</sub>O<sub>3</sub> addition up to 1.5 wt. % on the properties of aluminous cements containing MA spinel is investigated. The results showed that nano-Cr<sub>2</sub>O<sub>3</sub> addition has high effect on the phase composition, microstructure and then, properties of these cements. Hence, the amounts of spinel and CA<sub>2</sub> phases in the cement composition are increased with addition of nano-Cr<sub>2</sub>O<sub>3</sub>. On the other hand, the CA and C<sub>12</sub>A<sub>7</sub> amounts are decreased with increasing of nano-Cr<sub>2</sub>O<sub>3</sub>. On the other hand, the results revealed that C<sub>12</sub>A<sub>7</sub> phase is disappeared in cement composition containing 1.5 wt. % nano-Cr<sub>2</sub>O<sub>3</sub>. C<sub>12</sub>A<sub>7</sub> phase has low melting point and rapid initial and final setting times. Therefore, the setting times of cement pastes are increased with addition of nano-Cr<sub>2</sub>O<sub>3</sub>. Besides, the service temperature of these cements can shift to higher temperatures with addition of nano-Cr<sub>2</sub>O<sub>3</sub>. Hence, the slag corrosion resistance of refractory castables containing these cements is improved due to formation of higher spinel phase and disappearance of C<sub>12</sub>A<sub>7</sub> phase in the cement composition.

## REFERENCES

1. Banerjee, A., Das, S., Misra, S., Mukhopadhyay, S. Structural Analysis on Spinel (MgAl<sub>2</sub>O<sub>4</sub>) for Application in Spinel-bonded Castables *Ceramics International* 35 (1) 2009: pp. 381–390.
2. Khalil, N. M., Hassana, M. B., Ewaish, E. M. M., Saleha, F. A. Sintering, Mechanical and Refractory Properties of MA Spinel Prepared via Co-precipitation and Sol-gel Techniques *Journal of Alloys and Compound* 496 (1–2), 2010: pp. 600–607.
3. Díaz, L. A., Torrecillas, R. Hot Bending Strength and Creep Behavior at 1000–1400 °C of High Alumina Refractory Castables with Spinel, Periclase and Dolomite Additions, *Journal of the European Ceramic Society*, , 29 (1), 2009pp. 53–58. <http://dx.doi.org/10.1016/j.jeurceramsoc.2008.05.044>
4. Díaz, L. A., Torrecillas, R., de Aza, A. H., Pena, P., de Aza, S. Alumina-rich Refractory Concretes with Added Spinel, Periclase and Dolomite: A Comparative Study of Their Microstructural Evolution with Temperature *Journal of the European Ceramic Society* 25 (9) 2005: pp. 1499–1506.
5. Ganesha, I., Bhattacharjee, S., Sahaa, B. P., Johnsona, R., Rajeshwarib, K., Senguptab, R., Raob, M. V. R., Mahajana, Y. R. An Efficient MgAl<sub>2</sub>O<sub>4</sub> Spinel Additive for Improved Slag Erosion and Penetration Resistance of High-Al<sub>2</sub>O<sub>3</sub> and MgO–C Refractories *Ceramics International* 28 (3) 2002: pp. 245–253. [http://dx.doi.org/10.1016/S0272-8842\(01\)00086-4](http://dx.doi.org/10.1016/S0272-8842(01)00086-4)
6. Abo-El-Enain, S. A., Abou-Sekkina, M. M., Khalil, N. M., Shalma, O. A. Microstructure and Refractory

- Properties of Spinel Containing Castables *Ceramics International* 36 (5) 2010: pp. 1711–1717.
7. **Khalil, N. M. A., El-Hemaly, S. A. S., Girgis, L. G.** Aluminous Cements Containing Magnesium Aluminate Spinel from Egyptian Dolomite *Ceramics International* 27 (8) 2001: pp. 865–873.
  8. **de Aza, A. H., Pena, P., Rodriguez, M. A., Torrecillas, R., de Aza, S.** New Spinel-containing Refractory Cements *Journal of the European Ceramic Society* 23 (5) 2003: pp. 737–744.  
[http://dx.doi.org/10.1016/S0955-2219\(02\)00166-8](http://dx.doi.org/10.1016/S0955-2219(02)00166-8)
  9. **Lavat, A. E., Grasselli, M. C., Lovecchio, E. G.** Effect of  $\alpha$  and  $\gamma$  Polymorphs of Alumina on the Preparation of MgAl<sub>2</sub>O<sub>4</sub>-spinel-containing Refractory Cements *Ceramics International* 36 (1) 2010: pp. 15–21.  
<http://dx.doi.org/10.1016/j.ceramint.2009.06.015>
  10. **Pouyamehr, M. R., Nemati, Z. A., Faghihi Sani, M. A., Naghizadeh, R.** The Effect of Dolomite Type and Al<sub>2</sub>O<sub>3</sub> Content on the Phase Composition in Aluminous Cements Containing Spinel *Ceramics-Silikáty* 55 (2) 2011: pp. 169–175.
  11. **Zawrah, M. F.** Investigation of Lattice Constant, Sintering and Properties of Nano Mg–Al Spinels *Materials Science and Engineering A* 382 (1–2) 2004: pp. 362–370.
  12. **Ganesh, I., Bhattacharjee, S., Saha, B. P., Johnson, R., Mahajan, Y. R.** A New Sintering Aid for Magnesium Aluminate Spinel *Ceramics International* 27 (7) 2001: pp. 773–779.
  13. **Okuyama, Y., Kurita, N., Fukatsu, N.** Defect Structure of Alumina-rich Nonstoichiometric Magnesium Aluminate Spinel *Journal of Solid State Ionic* 177 (1–2) 2006: pp. 59–64.
  14. **Badiee, S. H., Otrroj, S., Rahmani, M.** The Effect of Nano-TiO<sub>2</sub> Addition on the Properties of Mullite-zirconia Composites Prepared by Slip Casting *Science of Sintering* 44 (3) 2012: pp. 341–354.
  15. **Badiee, S. H., Otrroj, S.** The Effect of Nano-titania Addition on the Properties of High-alumina Low-cement Self-flowing Refractory Castables *Ceramics-Silikáty* 55 (4) 2011: pp. 319–325.
  16. **Otrroj, S., Sagaeian, A., Daghighi, A., Nemati, Z. A.** The Effect of Nano-size Additives on the Electrical Conductivity of Matrix Suspension and Properties of Self-flowing Low-cement High Alumina Refractory Castables *Ceramics International* 36 (4) 2010: pp. 1411–1416.
  17. **Sarpoolaky, H., Zhang, S., Lee, W. E.** Corrosion of High Alumina and Near Stoichiometric Spinels in Iron-containing Silicate Slags *Journal of the European Ceramic Society* 23 (2) 2003: pp. 293–300.